

Remote Sensing of Atmospheric Particles Using LIDAR, Calipso Satellite, & AERONET: Algorithm Development

JAVIER MÈNDEZ¹, HAMED PARSIANI², EMMANUEL SANCHEZ³

Department of Electrical and Computer Engineer
University of Puerto Rico, Mayagüez (UPRM) Campus
PO Box 9000, Mayagüez , P.R. 00681-9000
PUERTO RICO

¹mjavier47@yahoo.com, ²parsiani@ece.uprm.edu³, ejsv.rum@gmail.com
<http://ece.uprm.edu/noaa-crest/>

Abstract: Algorithms have been developed for the determination of essential parameters such as Aerosol Size Distribution, Angstrom coefficient, and Single Scattering Albedo necessary in the determination of regional climatological model and weather prediction capabilities. The atmospheric power profile data for the calculations of these parameters have been obtained from Light Detection And Ranging (LIDAR) which is operational at City University of New York (CUNY). A similar system is near completion at the University of Puerto Rico at Mayaguez (UPRM). Also, the data from the Lidar in the orbit (CALIPSO satellite) has been used to calculate the Aerosol Optical Depth (AOD) for the western part of Puerto Rico and compare it to the AOD obtained from an AERONET network which is also located in the western region of Puerto Rico. The Calipso Lidar satellite transmits laser and collects backscattered light at two standard wavelengths (one wavelength at two polarizations). The AERONET network is a complementary method of determining the Optical Depth of the aerosol. The three aforementioned systems operate based on multiple wavelength laser light transmission and reception. Each system is explored in this paper, and full emphasis is given to the Lidar system which presently is near operation at the UPRM, explaining the functionality of the Laser, optical telescope, optics, sensors, signal processing systems, the power profile reflected from the aerosols are obtained at standard wavelengths of 355, 532, and 1064nms, both at CUNY and UPRM. The plots of aerosol distribution in the column of atmosphere in terms of the essential aerosol parameters have been produced using the Lidar data over New York urban area.

Keywords: Remote Sensing, Lidar, Calipso, AERONET, Atmospheric Parameters

1. Introduction

The fundamental issues that the globe is facing in terms of global warming, air quality, heat island effect, etc. must be attended by more accurately obtained data which will require high resolution land/ocean/atmosphere sensors organized as observational networks. These regional networks produce data related to climatological processes which at synoptic scale will bring about the understanding and prediction of global climate changes.

In this paper, three state of the art remote sensing methods are explored which are Lidar,

Calipso satellite, and AERONET. The working of each one of them is related to its ultimate climatological usefulness. The Lidar produces atmospheric power profile of the reflected light from the aerosols and clouds at different light wavelengths (normally at 355, 532, and 1064nms). This result is conducive to determination of aerosol parameters of the column of the atmosphere which may contain natural, urban, industrial, biomass burning, and marine aerosols.

Calipso satellite which became active Feb. 2007 has on board a Lidar (wavelengths of 355nm, and 532nm with dual polarizations)

which characterizes the aerosol parameters looking downward and acquiring data from its orbits around the globe.

On the other hand, AERONET (Aerosol Network) consists of a CIMEL sunphotometer device which allows the measurements of Aerosol Optical Depth (AOD) of atmosphere at its location. The daily AOD data obtained from its nine wavelengths and its calculated Aerosol Size Distribution (ASD) are made available to scientists world wide via AERONET.

In the subsequent sections, the system description of a typical Lidar (example: the Lidar under development at UPRM campus, and at CCNY campus, NY) is presented. Next, data obtained by Lidar over New York is processed by algorithms developed in MatLab to determine various aerosol parameters useful to the scientists in the climatological analysis, such as aerosol backscattering and extinction indices, and optical depth. Finally, the data of the Calipso Lidar and AERONET have been compared for the south western part of Puerto Rico during the same days and the results are presented.

2. Lidar System Description (at UPRM)

A Lidar such as the one which is being built at the UPRM campus, Fig. 1, has four fundamental subsystems: a laser, an optical telescope, receiving optics/sensors, and data acquisition/signal processing/display.

The laser is a Nd:YAG and consists of the three fundamental wavelengths of 355, 532, and 1064nm with energy pulses of 120mJ, 300mJ, 700mJ, and repeat rate of 20Hz with a pulse width of 6ns. Special high damage threshold guide mirrors are used for aligning of the laser beams into the atmosphere. Cassegrain telescope collects the backscatter light which is then separated by the optics according to wavelengths, and detected with photomultipliers (2 PMTs) and avalanche photodiode (1 APD). There are two PMT's to detect 355 and 532nm signals, and one APD for 1064nm. The data acquisition consists of a Licel transient recorder with three acquisition channels (one channel per sensor).

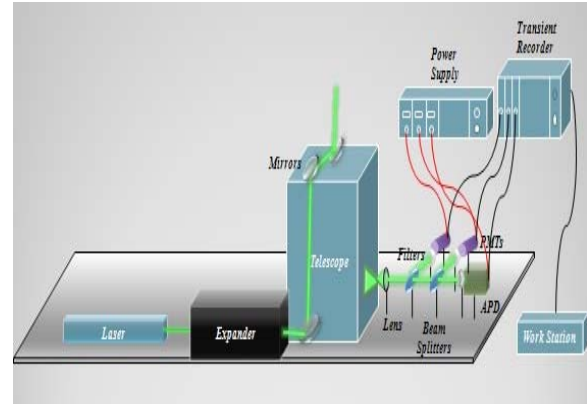


Figure 1: UPRM lidar system [1].

2.1 Lidar Data (at CCNY)

The CCNY Lidar data consist of the received signals at 355, 387, 407, 532, and 1064nm. The 387 and 407nm are Raman Channels (Inelastic) of 355nm. A typical data file received from Lidar (example CCNY Lidar) consists of 11 data columns. The first column is the atmospheric range. The next five columns are the received power intensity at 532, 355, 1064, 407, and 387nm measured in mV. The others five columns are equivalent to the previous five columns, but are measured in photon counting. The CCNY Lidar data used in this report is collected on May 15, 2007.

The analog power intensity data, in mv, is used in the testing of the algorithms developed in this paper, due its lower noise figure, as opposed to the photon counting data.

3. Data Processing Algorithm

The algorithm which is developed in Matlab loads the power profile data, extracts the column or columns from the data file, depending on the desired aerosol parameter calculations.

Next, the extracted data is filtered to reduce the noise caused by the sensors and nearby light sources.

3.1 Data Noise Attenuation & Adjustment

The mean for the first 3km of the digitalized data which represents the constant background noise is subtracted from the data, to attenuate the noise.

The received power signal is multiplied by square of the range (R^2) to have it range adjusted, which assumes the Lidar location has been altitude corrected as well. Figure 2 shows a comparison between the received raw signal, at 532 nm, and the signal with background noise attenuated. The noise filtered image of Fig. 2 shows more atmospheric details within the first one kilometer range. The comparison between the Lidar received signal range adjusted raw data and the same data noise filtered are clearly shown by Fig. 3.

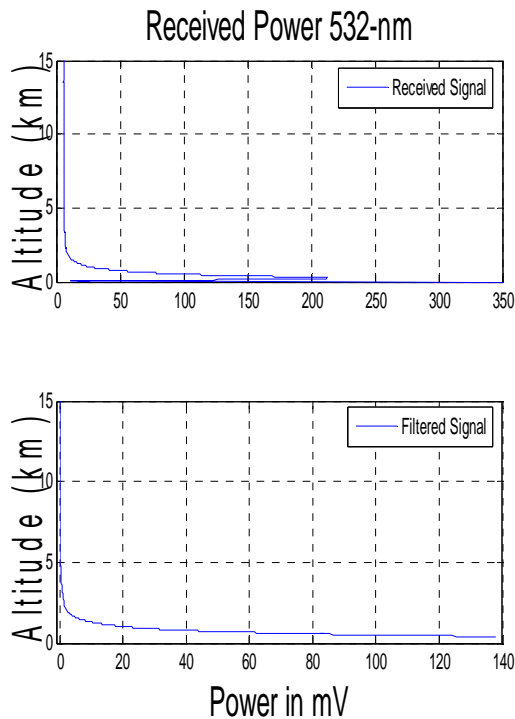


Figure 2: Raw received signal with background noise and the filtered signal

The corrected signal is important in the calculation of the aerosol extinction and backscatter coefficients. These two parameters are fundamental in the study of particles (or aerosols) present in the atmosphere. The aerosol optical depth or thickness and, aerosol size distribution are examples of parameter obtained using these two coefficients.

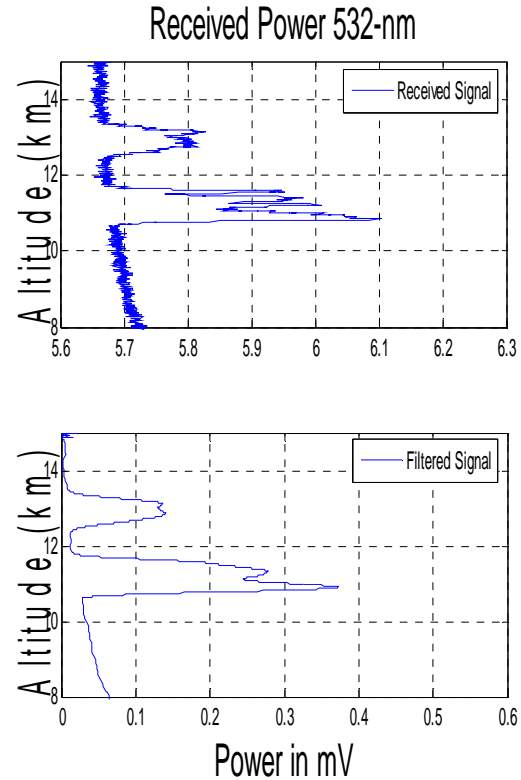


Figure 3: Range adjusted signal with and without noise

An intensity color coded image showing the received range adjusted, and noise attenuated, over many hours of Lidar observations is an essential image in portraying the atmospheric aerosol contents. Fig. 4 is the results of the MatLab plotting the logarithmic range adjusted power at 532 over 18 hours of observations.

In Fig. 4, clouds are present at altitudes between 10 and 14km. Specifically, at 2:46PM, in the first 3 Kms and the next 5 Kms, one could see the presence of smog and aerosols, respectively. The white points represent no data because the light had been absorbed or completely scattered by clouds.

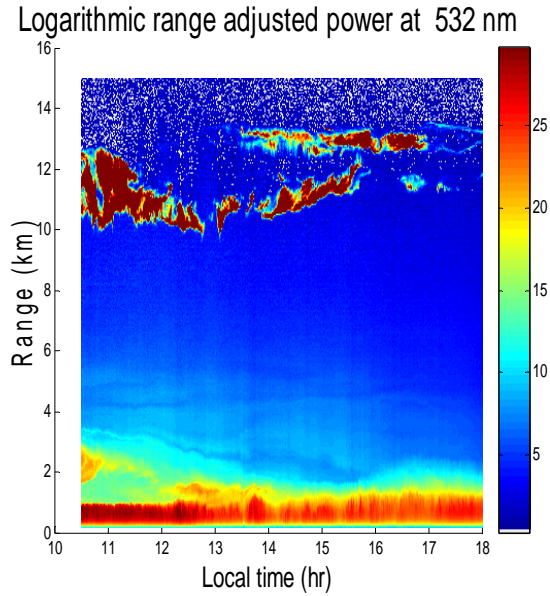


Figure 4: Logarithmic range adjusted raw power image at 532nm. In this image the clouds, aerosol layers, and NYC smog can be observed.

3.2 Backscatter and Extinction Coefficients

The backscattering coefficient (β) and the extinction coefficient (α) in Lidar signal processing must be determined by inverting the Lidar equation, but this is not possible in monostatic Lidars with only elastic channels, which requires solving two unknowns from a single received power equation.

The best method to invert the elastic Lidar equation to obtain the β is given by Klett Inversion Method [2]. This inversion assumes a simple relationship between the extinction and backscatter variables. This assumption leads to a stable analytical inversion of the equation for which Klett offers some empirical data to support the validity of the inverted solution in certain situations. Klett's solutions are computationally stable, and the method can improve the quality of Lidar images.

To determine the aerosol extinction and backscatter coefficients using the Klett method there is a need for molecular extinction and molecular backscatter coefficients. These coefficients are determined by applying the atmospheric assumptions or using the basic

meteorological data of temperature and pressure. With the determination of molecular coefficients, the elastic Lidar equation will depend only on the two independent quantities of aerosol extinction and aerosol backscatter. In the Klett method one assumes the aerosol extinction to backscatter ratio, known by aerosol Lidar ratio (S_a), which is a constant value under this assumption and can be estimated either from data tables or from other data [2, 3]. AERONET or portable sun-photometer can be used to obtain a good approximation to the actual value of the aerosol Lidar (S_a) [1,4].

The S_a is obtained, in this algorithm, by comparing the AOD calculated by Lidar data with AERONET AOD readings, or a portable sun-photometer. That is made possible by gradually changing the AOD calculated from Lidar data until the optical depth values match. Fig. 5 demonstrates the mentioned methodology and shows a value of 58 Sr was obtained for the particular Lidar data used.

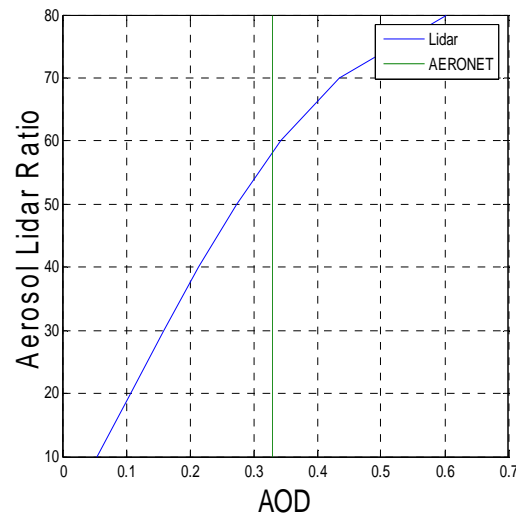


Figure 5: Real Lidar ratio determination using the AOD from Lidar and AERONET.

Fig. 6 shows the aerosol extinction and backscatter results with the Lidar Ratio of 58Sr.

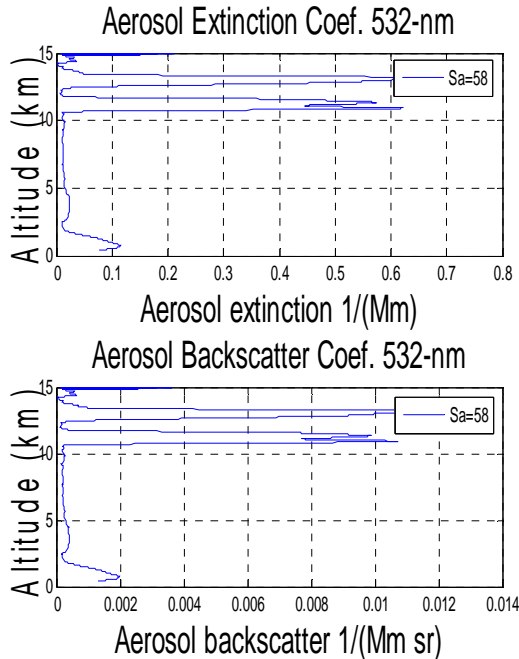


Figure 6: Aerosol extinction and backscatter coefficients using CCNY Lidar data at 2:46Pm.

Figures 7 and 8, show the images for aerosol extinction and backscatter, using CCNY Lidar data. A range adjusted power matrix was created to first obtain the image in Fig. 4 which was subsequently used to determine the extinction and backscatter plots for the available data time.

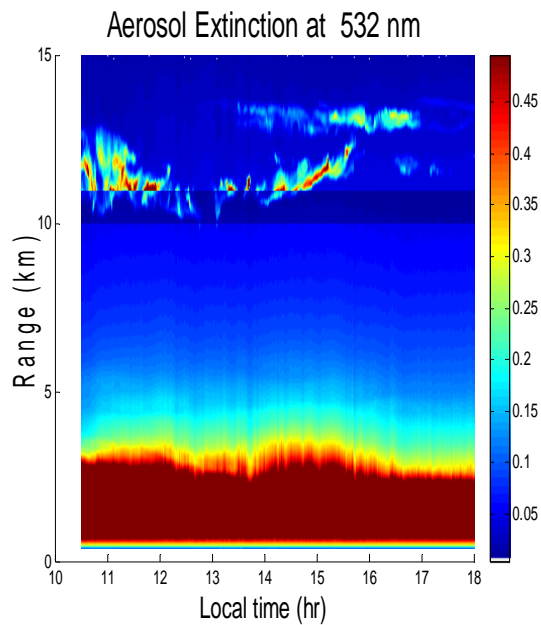


Figure 7: Aerosol Extinction image using CCNY Lidar data.

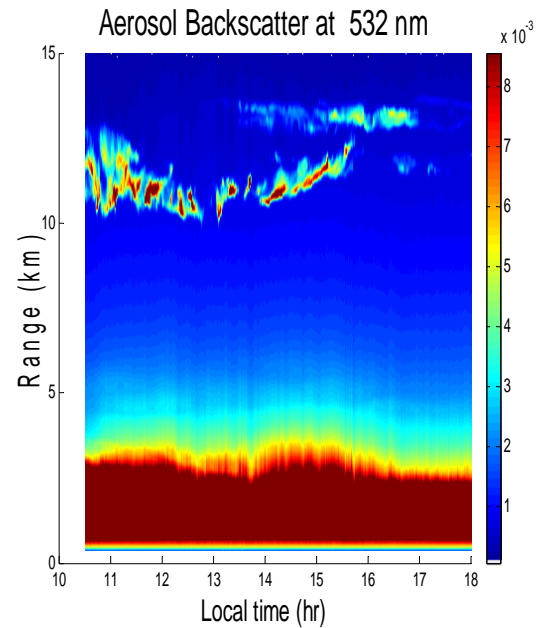


Figure 8: Aerosol Backscatter image Using CCNY Lidar data.

3.3 Aerosol Optical Depth (AOD)

AOD is a measure of transparency within a column of atmosphere containing layers of aerosols. Among the remote sensing equipment that are able to measure AOD are Lidar either land or satellite based, and CIMEL Sunphotometer (9 wavelengths and data is reported by AERONET). AOD could be measured by a portable Sunphotometer (using 5 to 7 wavelengths [4]).

The principle contaminant in the global warming is caused by CO₂ particles [5]. These and other contaminants cause a decrease in the AOD measure in the column of the atmosphere.

The AOD, an important warming index, is calculated using the extinction coefficient obtained from Lidar by integrating it as a function of range within the atmospheric column. Fig. 9 shows the AOD profile using the CCNY data of May 15, 2007.

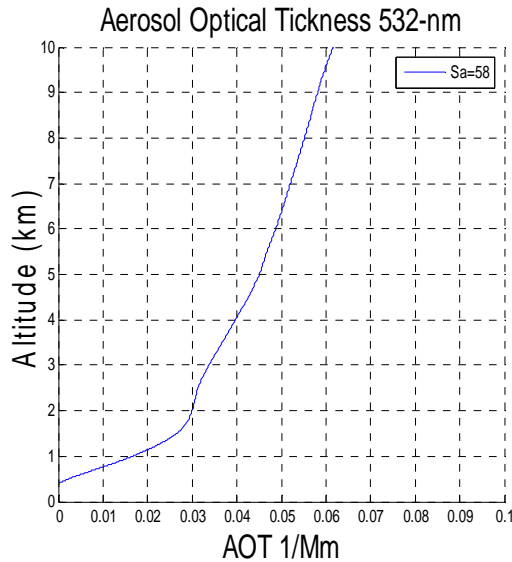


Figure 9: AOD at 532nm on May 15, 2007 at 2:46Pm in NYC.

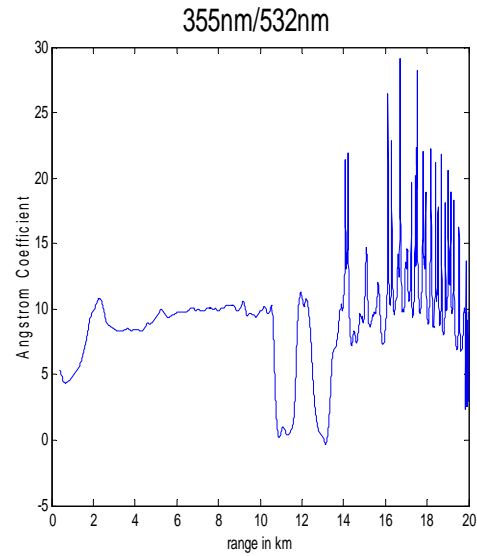


Figure 10: Angstrom coefficient using aerosol backscatter coefficient at 355nm and 532nm.

4 Angstrom Coefficient

Angstrom coefficient, Eq.1, describes the reliance of aerosol optical depth on wavelength. If the vertical stratified structures were cloud particles, the angstrom coefficient would be nearly close to zero and independent of the cloud optical depth since clouds are always made up of large particles. On the other hand, smoke plumes are made of very small absorbing particles, which are represented by a high angstrom coefficient [6].

$$angstrom = \frac{\log\left(\frac{\beta_{aer\ 532}}{\beta_{aer\ 355}}\right)}{\log\left(\frac{355}{532}\right)} \quad (1)$$

Figure 10 shows at 11km and 13km that the angstrom coefficient is close to zero, because of cloud presence at those altitudes. The high Angstrom coefficient at above 14 Km is indicative of smoke presence in those altitudes. High concentration of kinds at altitudes since 14km represents high Angstrom coefficient and indicatives smoke.

5 Single Scattering Albedo (SSA)

The SSA, w , is defined as the ratio of the scattering coefficient to the extinction coefficient, and measures the ratio of extinction by scattering, Q_{sca} , to total extinction during a single interaction of a photon beam with a particle. The SSA depends on the Mie-efficiencies for spherical shapes. The efficiencies depend on the refractive index n , the wavelength λ , and the particles radii r . The refractive index is a complex number where the imaginary part means absorption. The Extinction efficiency is the sum of scattering and absorption efficiencies. Eq. 2 and 3 show the scattering and absorption efficiencies [7].

$$Q_{sca.} = \frac{128\pi^4 r^4}{3\lambda^4} \left| \frac{n^2 - 1}{n^2 + 2} \right|^2 \quad (2)$$

$$Q_{abs} = \frac{8\pi}{\lambda} \text{Im} \left\{ \frac{n^2 - 1}{n^2 + 2} \right\} \left[1 - \frac{32\pi^3 r^3}{\lambda^3} \text{Im} \left\{ \frac{n^2 - 1}{n^2 + 2} \right\}^2 \right] \quad (3)$$

The ratio of the scattering coefficient to the sum of the scattering and absorption coefficients is then calculated to yield the scattering albedo, Eq.4. The SSA, then, indicates the percentage of atmospheric extinction due to scattering and absorption. An important point to be noted here is that the SSA provides a useful quantity as long as the scattering by aerosols is not very high. As the particles scattering reaches higher values, multiple scattering comes into play. Multiple scattering has been found to be small for visible wavelength lidar scattering from clean air or haze, but a large component in the presence of the fog or clouds.

$$w_0(\lambda) = \frac{Q_{sca}}{Q_{sca} + Q_{abs}} = \frac{Q_{sca}}{Q_{ext}} \quad (4)$$

Wavelength	Single Scattering Albedo
355nm	0.5099
532nm	0.3322
1064nm	0.1579

Table 1 SSA using Mie theory for spherical aerosols.

Wavelength	Aerosol Optical Depth
355nm	0.3261
532nm	0.2063
1064nm	0.0286

Table 2 AOD at the three fundamental wavelength, using CCNY lidar data on May 15, 2007 at 2:46Pm.

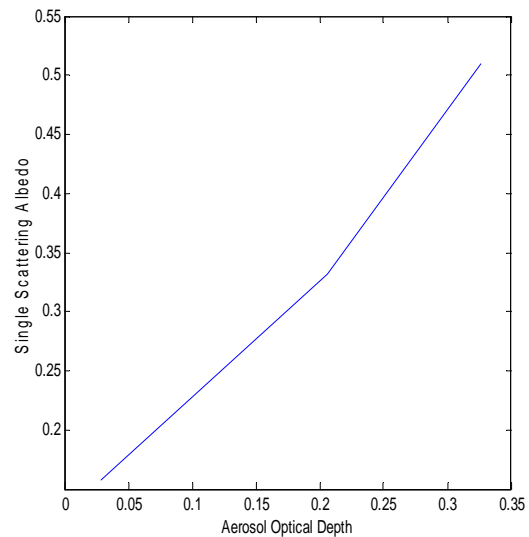


Figure 11: shows that the SSA is proportional to the AOD. If the AOD decreases the percent of light scattered (SSA) decreases too, causing global warming.

6 Aerosol Size Distribution (ASD)

The range of the size distribution for atmospheric aerosols varies from 50nm to 15µm radius. The aerosols studied in this publication have been assumed spherical, this assumption has been made for the calculation of efficiencies for aerosol extinction and backscatter coefficients.

The ASD for a column of atmosphere could be determined using instruments such as the SPM and AERONET. However, AERONET provides a single ASD for a vertical column of atmosphere. Lidar provides a comprehensive ASD profile which represents ASD at different heights. The ASD can be obtained from the backscatter and extinction coefficients at the specific altitude.

Figure 12 shows the vertical profile of the ASD measured in the column from 40m to 2.5 km. This distribution has been determined using the combination of aerosol extinction and backscatter coefficient of the three fundamental wavelengths at the mentioned column. The extinction and backscatter coefficients data as a function of altitude was used to retrieve aerosol microphysical parameters through inversion with regularization [8].

Figure 13 shows the effective radius at different altitudes for the same column of data. To determine the effective radius the ASD has been determined at the same attitude. In this atmospheric column the effective radius is determined to be between 0.1 and 0.24 μm . Large particles are present in the observed column which correspond to the middle of the Planetary Boundary Layer (PBL).

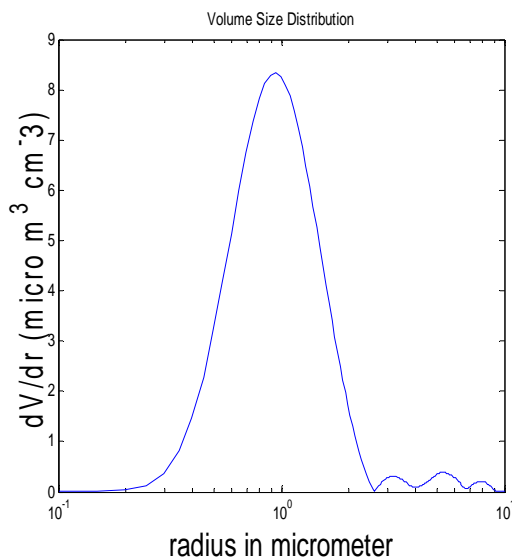


Figure 12: ASD retrieved from CCNY Lidar on 15 May 2007.

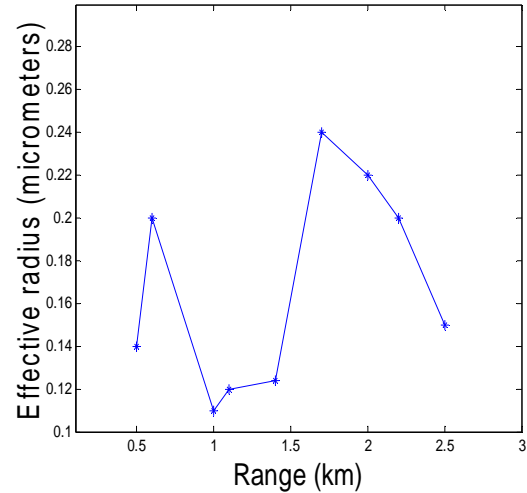


Figure 13: Effective radius at different altitudes.

It is possible to validate ASD with in-situ Sun-photometer data, but as shown in [4], it requires a Neural Network to take the SPM data and convert it to ASD data after it has been trained with AERONET data. The Neural Network application could be simply done by using MatLab Neural Network tool box as has been implemented by [1,9].

7. Calipso-AERONET comparison for AOD measurements

Efforts were made to compare the AOD measurements of Calipso Lidar, Fig. 14, with AERONET. The result is as depicted in the Table-3. For the most part, Calipso data agreed with the values reported by AERONET but, occasionally, a substantial difference was observed. Since Calipso overpass is about 40km away from La Parguera (home of AERONET), the trade winds and clouds could play a role in the AERONET/Calipso discrepancy.

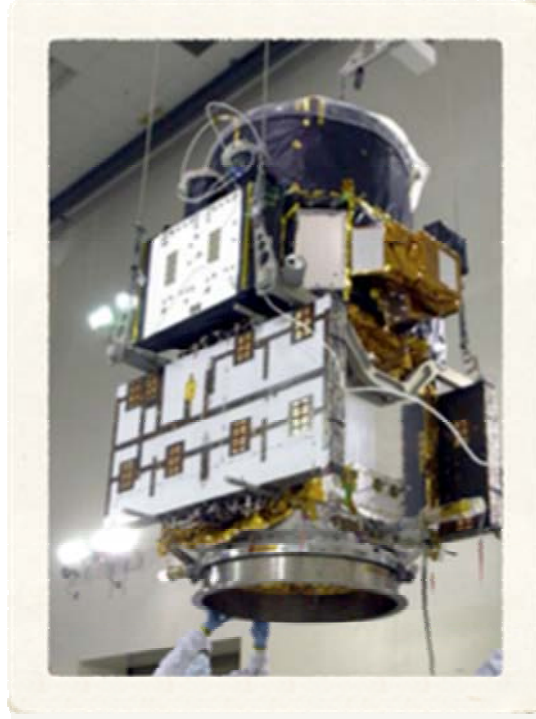


Fig. 14: Calipso Lidar on board Calipso Satellite with 532nm dual polarization & 1064nm

	CALIPSO	AERONET	Error
Day	AOD	AOD	
Jan 6, 2008	0.077	0.070	9.252
Jan 30, 2008	0.132	0.122	7.499
Feb 7, 2008	0.094	0.063	33.127
Aug 1, 2008	0.238	0.259	8.824
Aug 8, 2008	0.295	0.390	32.265
Aug 17, 2008	0.277	0.300	8.134
Aug 25, 2008	0.094	0.081	13.462
Sep 2, 2008	0.195	0.213	9.007

Table 3: Calipso-AERONET comparison for AOD measurement over western part of Puerto Rico

5 Conclusions

Remote sensing sensors such as land based Lidar, Calipso satellite, CIMEL Sunphotometer are a few examples of important devices to be networked for observation of the regional climatological variations. In this paper, the working of the Lidar system and the usage of the same in terms of determination of important parameters for climatological variations and predictions were presented. CCNY Lidar data was used as test bed data for the determination of the aerosol parameters. Essential among these parameters determined and plotted were Aerosol Size distribution, Angstrom coefficient, and Single Scattering Albedo.

Calipso Lidar was compared for a few days with AERONET readings of AOD. This result showed a reasonable match between the two on a few days and some large discrepancies in other days. It is important to note that the foot-print of Calipso orbit to the location of AERONET was about 40 Km, and the AOD discrepancies may have been caused by large atmospheric differences in aerosols and clouds over the two regions.

6 Acknowledgements

The authors appreciate the support of NOAA CREST under grant NA17AE1625. This project was also partially supported by NASA-EPSCOR, NASA-PASSER, and UPRM. The views, opinions, and findings contained in this report are those of the authors and should not be construed as an official National Oceanic and Atmospheric Administration or U.S. Government position, policy, or decision.

Also special thanks to:

- CCNY Lidar Staff.
- UPRM students: Mariano Martes & Allan Lizarraga

References

- [1] Hamed Parsiani and Javier Méndez,, “Aerosol Size Distribution using Lidar Data and a Typical Lidar Assembly”, **WSEAS** Transactions on Systems, Issue 11, Volume 7, Nov., 2008.
- [2] James D. Klett, Stable Analytical Inversion Solution for Processing Lidar Returns, Optical Society of America, Applied Optics/Vol. 20, No. 2/ Applied Optics/ 15 January 1981
- [3] Federick G. Fernald, Analysis of Atmospheric Lidar Observations, Optical Society of America, Applied Optics/Vol. 23, No. 5/1 March 1984.
- [4] Hamed Parsiani, Andres Bonilla, “Aerosol Size Distribution Estimation using Sun photometer and Artificial Neural Network,” 12th **WSEAS** International Conference on SYSTEMS, Heraklion, Greece, July 22-24, 2008.
- [5] Jill A. Engel-Coxa, Raymond M. Hoff b, Raymond Rogersb, Fred Dimmickc, Alan C. Rushc, James J. Szykmand, Jassim Al-Saadie, D. Allen Chub, Erica R. Zella aBattelle, “Integrating lidar and satellite optical depth with ambient monitoring for 3-dimensional particulate characterization”, 2006.
- [6] J.L Guerrero, B. Ruiz, and L. Alados, "Multi spectral Lidar Characterization of the Vertical Structure Saharan Dust Aerosol over Southern Spain", December 21, 2007.
- [7] C. F. Bohren and D. R. Huffman, "Absorption and scattering of light by small particles", pp. 135-136, (Wiley, New York, 1983)
- [8] Albert Ansmann and Detlef Müller, “Lidar and Atmospheric Aerosol Particles,” Optical Sciences, 2005.
- [9] YELDA OZEL , IRFAN GUNNEY , EMIN ARCA, “Neural Network Solution to the Cogeneration System by Using Coal,” 12th **WSEAS** International Conference on CIRCUITS, Heraklion, Greece, July 22-24, 2008.